

## Multi-scale and multi-pathways: How the ULF waves hoard electrons into precipitation

Dmitri Vainchtein\*, Xiaojia Zhang†, and Anton Artemyev†  
 \*Nyheim Plasma Institute, Drexel University, Philadelphia, USA  
 †University of California, Los Angeles, USA

*Summary.* The nonlinear resonant electron scattering by whistler-mode chorus waves is one of the main drivers of the electron precipitation into the Earth's atmosphere. However, the electron precipitation shows signs of modulation by much slower ultra-low-frequency (ULF) waves, that cannot be in resonance with electrons. In this presentation we use the Hamiltonian frameworks for slow-fast systems to consider two-pronged impact of the ULF waves on the electrons' dynamics: First, ULF waves modulate the whistler waves; and second, ULF waves directly affect electron distribution functions. We implement THEMIS observations of ULF waves and modulated whistler waves to perform numerical simulations of electron dynamics. We show how the quasi-linear and nonlinear regimes of electron scattering by whistlers interchange within one ULF period and how this interplay of the two regimes affect the electron scattering (precipitation) rates.

### Ultra-low-frequency (ULF) and whistler waves in the Earth magnetosphere

Ultra-low-frequency (ULF, 0.001–1 Hz) perturbations are generated at the magnetopause and propagate into the inner magnetosphere, and effectively modulate whistler waves. Close to the magnetopause, VLF wave bursts have the same periodicity as the ULF perturbations. Our results demonstrate that almost the entire outer magnetosphere (from the geostationary orbit to most elliptical orbits), including the outer radiation belts, is significantly influenced by ULF perturbations excited by magnetopause dynamic responses to the solar wind. Space observations show that ULF wave modulate not only whistler intensity, but also pitch-angle distributions of electrons. ULF waves propagate with velocities much smaller than electron thermal velocity. Therefore the interaction of ULF waves with electrons is non-resonant (in this proposal we do not consider the azimuthal resonances effective mostly for relativistic electrons). This interaction causes quasi-periodic changes of characteristic pitch-angle of distribution functions. We use conservation of the electron adiabatic invariants (the magnetic moment and the second adiabatic invariant) to describe the evolution of electron distributions. We will fit spacecraft measurements of electron distributions in the 1-100 keV energy range, and rewrite this fitted distribution in terms of adiabatic invariants. With ULF magnetic field included in calculation of invariants, we compute electron distribution for several time moments within one ULF wave period.

### The nonlinear wave-particle interaction

Consider a relativistic electron interacting with a whistler wave propagating at an arbitrary angle  $\theta$  relative to the background magnetic field. In the absence of the resonance overlapping, which is the most typical situation in the inner magnetosphere, the corresponding Hamiltonian is

$$H = m_e c^2 \gamma + \frac{e B_w}{k_{\parallel} \gamma} \sum_{n=0, \pm 1, \dots} h^{(n)} \sin(\phi + n\psi), \quad \gamma = \sqrt{1 + \frac{p_{\parallel}^2}{m_e^2 c^2} + \frac{2\mu\Omega_{ce}}{m_e c^2}} \quad (1)$$

In (1),  $n$  is a harmonic number, function  $h^{(n)}(\mu, \theta, s, p_{\parallel})$  defines the effective wave amplitude for a particular harmonic [1],  $(s, p_{\parallel})$  are field-aligned coordinate and momentum,  $(\psi, \mu)$  are gyrophase and magnetic moment ( $\mu = p_{\perp}^2 / 2m_e \Omega_{ce}$ ),  $\Omega_{ce} = \Omega_{ce}(s)$  is an electron gyrofrequency,  $\phi, k_{\parallel}(s)$ , and  $\omega(t)$  are a wave phase, field-aligned wave vector component, and wave frequency. Particle energy  $E \approx H - m_e c^2 = m_e c^2 (\gamma - 1)$ , magnetic moment  $\mu = \mu(\gamma, \alpha)$  is defined by  $\gamma$  and particle equatorial pitch-angle  $\alpha$ . Wave amplitude  $B_w$  is much smaller than a typical particle energy ( $e B_w / k \ll E$ ).

Dynamics of particles governed by Eq.(1) includes nonlinear resonant scattering and trapping, cite Omura, Artemyev. Nonlinear scattering occurs at almost every resonant interaction and produces changes of the electron energy and pitch-angle,  $\Delta^S E$  and  $\Delta^S \alpha$ , see Fig. 1(a,b). Such changes cause a drift in the energy/pitch-angle space, directed towards relatively small values of  $E$  and  $\alpha$ . This drift cannot be described by the quasi-linear diffusion. Not every resonant particle is scattered, though, but some of them are trapped. Particle trapping (such as the one occurring at about  $t = 90$  in Fig. 1(a,b)) results in significant changes of the energy and pitch-angle,  $\Delta^P E, \Delta^P \alpha$ . Such changes are much stronger than any individual change due to scattering, but the number of particles trapped at a single resonance crossing is much smaller than the number of scattered particles. The relative amount of resonant particles (with a given energy and pitch-angle) being trapped during a given resonant interaction is called *probability of trapping*.

### Probabilistic approach: a single wave

Consider a 2D space  $(E, \alpha)$  with a discretization  $(i, j)$ , i.e., the electron distribution function  $f(E, \alpha)$  is defined as  $f_{ij} = f(E_i, \alpha_j)$ . We can introduce the quantity  $s_{mn}^{kl}(W)$  as a probability of a particle to move from the state  $(E_k, \alpha_l)$  to the state  $(E_m, \alpha_n)$  due to a single scattering with a given wave. The letter  $W$  indicates all the relevant wave's characteristics, most importantly the amplitude, the frequency, and the angle of the wave propagation. For each concrete wave, one can

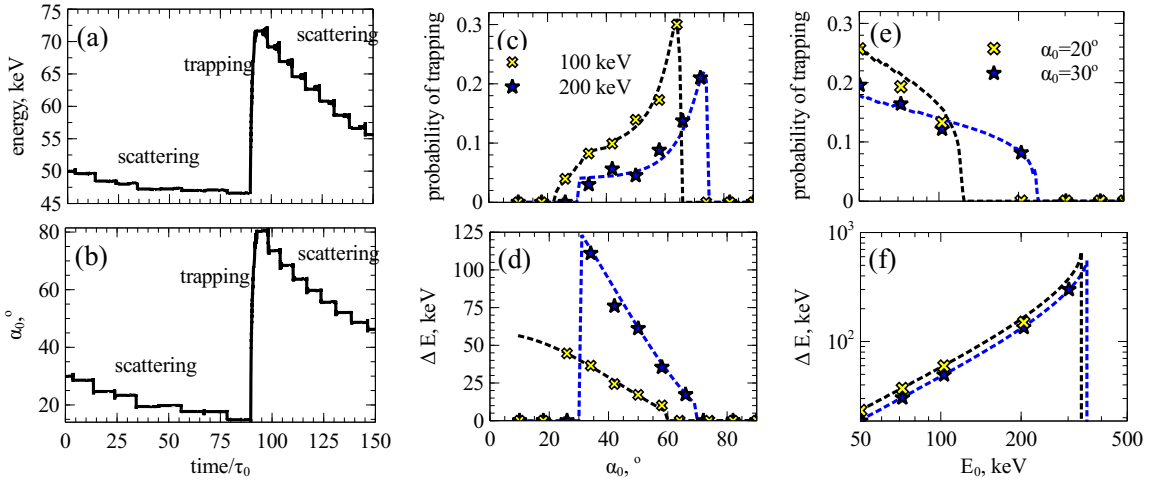


Figure 1: (a,b) A fragment of a 100 keV electron trajectory: electron energy (panel (a)) and pitch-angle (panel (b)). This fragment includes several scattering and one trapping. Time is normalized by a typical bounce period  $\tau_0 = LR_E/c \sim 1/7s$  ( $R_E$  is the Earth radius). (c-f) Main characteristics of electron trapping by oblique (c,d) and parallel (e, f) waves. Analytic results (curves) are shown together with test particle simulations (symbols): energy change in trapping  $\Delta^P E$  and the probability of trapping for various initial energy  $E_0$  and pitch-angle  $\alpha_0$ .

view all  $s_{mn}^{kl}(W)$  as the elements of a big 4D matrix, that defines the phase space transport due to scattering. Similarly, we can introduce the probability for trapping in the same way as we did for scattering:  $p_{mn}^{kl}(W)$  is a probability of a particle to move from the state  $(E_k, \alpha_l)$  to the state  $(E_m, \alpha_n)$  due to a single trapping into resonance with a given wave. Almost all of the matrix elements are zero. Thus we arrive at

$$\frac{\partial f_{ij}}{\partial t} = -\frac{2}{\tau_{ij}} f_{ij} + \sum_{kl} R_{ij}^{kl}(W) f_{kl}; \quad R_{ij}^{kl}(W) = \frac{N_{kl}}{\tau_{kl}} (s_{ij}^{kl}(W) + p_{ij}^{kl}(W)) \quad (2)$$

where each  $\tau_{ij} = \tau(E_i, \alpha_j)$  is the bounce period. Elements of  $R_{ij}^{kl}(W)$  depend on wave characteristics. There is a noticeable difference between  $s_{mn}^{kl}(W)$  and  $p_{mn}^{kl}(W)$ : while the non-zero elements of  $s_{mn}^{kl}(W)$  correspond to nearby cells (around  $k = m, l = n$ ), the elements of  $p_{mn}^{kl}(W)$  are somewhat removed from there. Note that Eq. (2) is linear with respect to the distribution function  $f_{ij}$ , and nonlinear with respect to properties of the wave,  $W$ . The nonlinearity is included in the array  $R_{ij}^{kl}(W)$ .

### Multiple waves

For an ensemble of waves, let  $\rho(W)$  define the statistical weight of a certain set of parameters,  $\rho(W)$  describes statistics of the wave amplitude  $B_w$  and frequency  $\omega$ ). The distribution  $\rho(W)$  is normalized so that  $\int \rho(W) dW = T_{int}/T_{tot}$  where  $T_{tot}$  is the total duration of spacecraft measurements and  $T_{int}$  is a cumulative duration of observations of intense waves. Normalized  $\rho(W)$  gives a

$$\frac{\partial f_{ij}}{\partial t} = -\frac{n_{ij}}{\tau_{ij}} \frac{T_{int}}{T_{tot}} f_{ij} + \sum_{kl} \left( \int_W R_{ij}^{kl}(W) \rho(W) dW \right) f_{kl} = -\frac{n_{ij}}{\tau_{ij}} \frac{T_{int}}{T_{tot}} f_{ij} + \sum_{kl} \langle R_{ij}^{kl} \rangle f_{kl} \quad (3)$$

where  $\langle R_{ij}^{kl} \rangle = \int_W R_{ij}^{kl}(W) \rho(W) dW$ . For a given state  $(E_i, \alpha_j)$ ,  $\langle R_{ij}^{kl} \rangle$  contains two groups of nonzero elements in the  $(E, \alpha)$  space. The elements located near the ‘‘target’’ cell describe the efficiency of scattering, which, for the first cyclotron resonance, results in energy/pitch-angle decrease. The elements related to trapping are located relatively far from the ‘‘target’’ and they correspond to energy/pitch-angle increase.

### Conclusions

The objective of the current research was to describe how the ULF waves impact the dynamics of electrons in the Earth magnetosphere: directly through the non-resonant interaction, and indirectly through modulating the whistler waves, that do have the non-linear resonance interaction with electrons. The research was supported in part by the NASA award 80NSSC19K0266.

### References

- [1] Tao, X., Bortnik, J., (2010). Nonlinear interactions between relativistic radiation belt electrons and oblique whistler mode waves. *Nonlinear Processes in Geophysics* **17**:599–604.
- [2] Artemyev, A. V. et al., (2014). Electron scattering and nonlinear trapping by oblique whistler waves: The critical wave intensity for nonlinear effects. *Physics of Plasmas* **21**:102903.
- [3] Nunn, D., Omura, Y., (2015). A computational and theoretical investigation of nonlinear waveparticle interactions in oblique whistlers. *J. Geophys. Res.* **120**:2890–2911.